

Published in final edited form as:

Nat Neurosci. 2009 July ; 12(7): 857–863. doi:10.1038/nn.2334.

NADPH oxidase is the primary source of superoxide induced by NMDA receptor activation

Angela M Brennan¹, Sang Won Suh¹, Seok Joon Won¹, Purnima Narasimhan², Tiina M Kauppinen¹, Hokyoo Lee¹, Ylva Edling¹, Pak H Chan², and Raymond A Swanson¹

¹Department of Neurology, University of California, San Francisco and Veterans Affairs Medical Center, San Francisco, California, USA.

²Departments of Neurosurgery, Neurology and Neurological Sciences, and the Program in Neurosciences, Stanford University School of Medicine, Stanford, California, USA.

Abstract

Neuronal NMDA receptor (NMDAR) activation leads to the formation of superoxide, which normally acts in cell signaling. With extensive NMDAR activation, the resulting superoxide production leads to neuronal death. It is widely held that NMDA-induced superoxide production originates from the mitochondria, but definitive evidence for this is lacking. We evaluated the role of the cytoplasmic enzyme NADPH oxidase in NMDA-induced superoxide production. Neurons in culture and in mouse hippocampus responded to NMDA with a rapid increase in superoxide production, followed by neuronal death. These events were blocked by the NADPH oxidase inhibitor apocynin and in neurons lacking the p47^{phox} subunit, which is required for NADPH oxidase assembly. Superoxide production was also blocked by inhibiting the hexose monophosphate shunt, which regenerates the NADPH substrate, and by inhibiting protein kinase C zeta, which activates the NADPH oxidase complex. These findings identify NADPH oxidase as the primary source of NMDA-induced superoxide production.

Activation of the neuronal NMDAR initiates several downstream events, including cation influx, activation of nitric oxide synthase and formation of superoxide^{1–3}. Superoxide functions as an inter-cellular messenger in long-term potentiation^{4,5} and participates in redox inhibition of NMDAR channel function⁶; however, superoxide can also promote neuronal death when NMDAR activation is sustained^{1,7}. Notably, the primary source of superoxide induced by NMDAR activation remains unresolved.

Initial studies suggested a mechanism in which Ca²⁺ influx through NMDAR channels leads to mitochondrial depolarization^{8,9} and subsequent mitochondrial production of superoxide^{10,11}. However, a biochemical mechanism linking these events has not been identified and evidence supporting mitochondria as the primary source of neuronal superoxide production remains indirect^{12,13}. Calcium was shown to induce superoxide production in isolated

© 2009 Nature America, Inc. All rights reserved.

Correspondence should be addressed to R.A.S. (Raymond.swanson@ucsf.edu).

AUTHOR CONTRIBUTIONS

A.M.B. carried out the cell culture studies and data analysis and prepared the manuscript drafts. S.W.S. supervised the mouse surgical studies and analyzed these data. S.J.W. performed mouse surgery studies and mouse brain histology. P.N. maintained the *Sod2*⁺ mouse colony and prepared the *Sod2*⁺ cell cultures. T.M.K. and Y.E. assisted with the p47^{phox} translocation studies and data analysis. H.L. assisted in the analysis of the cell culture ethidium fluorescence results. P.H.C. assisted with the studies involving *Sod2*⁺ neurons. R.A.S. organized the studies and prepared the final manuscript.

Note: Supplementary information is available on the Nature Neuroscience website.

Reprints and permissions information is available online at <http://www.nature.com/reprintsandpermissions/>

mitochondria¹⁴, but more recent studies indicate that this effect is highly dependent on experimental conditions, especially the presence of bovine serum albumin in the medium and succinate as a metabolic substrate¹³. The important question is whether mitochondria *in situ* show an increase in superoxide production during NMDAR activation. In support of this, studies using cationic, oxidant-sensitive fluorescent indicators have found an increase in fluorescent signal in neuronal mitochondria after NMDAR activation^{10,11,15}. However, this mitochondrial localization does not distinguish between intra- and extra-mitochondrial sources of oxidant production. Moreover, studies using inhibitors of mitochondrial electron transport to block mitochondrial superoxide production are confounded by the fact that the inhibitors also cause mitochondrial depolarization, and thus reduced uptake of the cationic indicators¹⁶.

An alternate source of superoxide, also activated by Ca^{2+} influx, is NADPH oxidase. NADPH oxidase is a cytoplasmic enzyme that transfers an electron from NADPH to molecular oxygen to generate superoxide. NADPH oxidase was originally described in neutrophils, but has subsequently been identified in many other cell types including neurons^{17,18}. NADPH oxidase is composed of catalytic and regulatory subunits that, on activation, translocate and coalesce with an assembly subunit at a plasma or luminal membrane. Neurons and neutrophils express the NOX2 isoform of NADPH oxidase, which contains the gp91 catalytic subunit and requires the p47^{phox} assembly subunit¹⁷. Neurons may also express the NOX1 and NOX4 isoforms, both of which may also require p47^{phox} in some cell types¹⁷.

Here, we evaluated the role of NADPH oxidase in the neuronal production of superoxide induced by NMDAR activation. We found a near-complete absence of superoxide production in neurons lacking functional NADPH oxidase and in neurons in which NADPH oxidase function had been inhibited, along with markedly reduced NMDA neurotoxicity under these conditions. Our results indicate that NADPH oxidase is the primary source of superoxide production following neuronal NMDAR activation.

RESULTS

NMDAR activation induces superoxide production by NOX

We evaluated neuronal superoxide production by measuring intra-cellular accumulation of oxidized dihydroethidium (dHEth) in mouse cortical neuronal cultures that were preloaded with dHEth. dHEth is oxidized by superoxide or oxidant metabolites of superoxide to form fluorescent ethidium and related species, which are trapped in cells by DNA binding^{10,19–22}. Real-time fluorescence imaging showed that NMDA induced a rapid increase in ethidium fluorescence that plateaued after 20–30 min (Fig. 1a), which is consistent with prior reports^{10,15}. We obtained similar results in experiments performed at 35 °C or 21–25 °C, and all subsequent experiments were carried out at room temperature with images acquired 30 min after the addition of NMDA. Under these conditions, NMDA produced a roughly threefold increase in the number of neurons with detectable ethidium fluorescence (Fig. 1b,c). This increase was blocked by the oxidant scavenger Trolox and mimicked by H_2O_2 , indicating that it was oxidant induced. The NMDA-induced signal was also blocked in Ca^{2+} -free medium and by MK801, which is consistent with it being the result of an NMDAR-mediated process, and was not blocked by 6-cyano-7-nitroquinoxaline-2,3-dione (CNQX), thus excluding an effect of NMDA-induced glutamate release acting on AMPA/kainate receptors. Notably, the NMDA-induced signal was also completely blocked by apocynin, a methoxy-substituted catechol that blocks NOX2 assembly, but does not inhibit mitochondrial dehydrogenases²³. NADPH oxidase generates superoxide using NADPH formed by the hexose monophosphate shunt. Neurons incubated with an inhibitor of this pathway, 6-aminonicotinamide (6AN)^{21,24,25} showed no increase in ethidium fluorescence after NMDA exposure.

We also examined superoxide production in neurons prepared from *Ncf1*^{-/-} (also known as *p47^{phox}*) mice to confirm the role of NADPH oxidase in NMDA-induced superoxide production. Cells from *p47^{phox}*^{-/-} mice are unable to assemble a NOX2 NADPH oxidase complex^{21,26}. *p47^{phox}*^{-/-} neurons showed a very attenuated NMDA-induced ethidium signal relative to wild-type neurons (Fig. 1d,e). When incubated with H₂O₂, however, *p47^{phox}*^{-/-} neurons had ethidium fluorescence that was comparable to that produced in wild-type neurons, thus excluding any difference in dHEth loading or metabolism in the *p47^{phox}*^{-/-} cells.

We corroborated the ethidium fluorescence results by immunostaining for the lipid peroxidation product 4-hydroxynonenal (4HNE)²⁷. Neurons treated with NMDA showed an increase in 4HNE immuno-reactivity that was blocked by Trolox, apocynin or 6AN, and in cultures prepared from *p47^{phox}*^{-/-} mice (Fig. 2). Together, these results indicate that NADPH oxidase is the primary source of NMDA-induced superoxide production.

Role of mitochondria in NMDA-induced superoxide production

Studies using oxidant-sensitive dyes have suggested that mitochondria are a major source of superoxide formation during NMDAR activation^{10,11,15}; however, mitochondrial accumulation of the oxidized dyes results from their positive charge and does not exclude oxidant production from an extra-mitochondrial source. Here we distinguished between mitochondrial and NADPH oxidase-derived superoxide production on the basis that both glucose and non-glucose substrates support mitochondrial respiration (and thus mitochondrial superoxide production), but only glucose can support the regeneration of NADPH required for NADPH oxidase activity. Neurons maintained comparable ATP concentrations when incubated with either glucose or pyruvate (Fig. 3a), consistent with the capacity of neurons to utilize pyruvate for oxidative energy metabolism. However, the NMDA-induced ethidium signal was not observed when the cultures were supplied with pyruvate alone (Fig. 3b). This result cannot be attributed to superoxide scavenging by pyruvate because pyruvate did not suppress the NMDA-induced signal produced in presence of glucose (Fig. 3b). Moreover, the concentration of pyruvate used in these studies (1 mM) had no detectable effect on dHEth oxidation by exogenous H₂O₂ (Supplementary Fig. 1 online). Lactate was also found to support neuronal energy metabolism, but did not support NMDA-induced superoxide production (data not shown). Conversely, we found no reduction in NMDA-induced ethidium fluorescence when we blocked pyruvate transport into mitochondria with 4-hydroxycyanocinnamate (250 μM) or the glycolytic inhibitor iodoacetate (250 μM)²¹ (Supplementary Fig. 1).

We carried out additional experiments to confirm that ethidium fluorescence measurements would be capable of detecting superoxide produced by mitochondria, if this occurred. Neurons incubated with either the complex III inhibitor antimycin²⁸ or the protonophore *p*-trifluoromethoxy carbonyl cyanide phenyl hydrazone (FCCP)¹⁰ showed a two- to three-fold elevation in ethidium fluorescence (Fig. 3c–f), with or without the added presence of oligomycin to prevent ATP consumption by mitochondrial ATP synthase⁹. The ethidium signal induced by these agents was undiminished in neurons treated with 500 μM apocynin and in neurons prepared from *p47^{phox}*^{-/-} mice (Fig. 3e,g), confirming that these conditions do not interfere with the detection of superoxide produced by mitochondria (Fig. 3g). We also prepared neurons from mice that had a twofold overexpression of mitochondrial superoxide dismutase (*Sod2*⁺ mice²⁹). The NMDA-induced ethidium responses were not substantially different in neurons prepared from *Sod2*⁺ mice than from wild-type littermate controls (Fig. 3h). There was, however, a significant decrease in ethidium fluorescence in the *Sod2*⁺ neurons when treated with antimycin and oligomycin (*P* < 0.05), which is consistent with an increased capacity for mitochondrial superoxide scavenging.

We also considered other potential sources of superoxide. Nitric oxide synthase (NOS) and xanthine oxidase can both generate superoxide^{30,31}, and NOS, similar to NADPH oxidase, is

ultimately dependent on glucose for NADPH substrate. However, neurons treated with either allopurinol or gallic acid to inhibit xanthine oxidase³² or *N*_ω-nitro-L-arginine methyl ester hydrochloride (L-NAME) to inhibit NOS³³ showed no reduction in NMDA-induced ethidium fluorescence (Supplementary Fig. 2 online).

Prior studies have shown that activation of synaptic and extra-synaptic NMDARs can have differing effects³⁴. We found that transient activation of synaptic NMDAR with bicuculline and 4-aminopyridine produced time-linked spikes in intracellular calcium and an increase in ethidium fluorescence (Supplementary Fig. 3 online), suggesting that synaptic NMDAR activation is sufficient to activate NADPH oxidase. Synaptic NMDARs were then blocked with MK801, administered with bicuculline and 4-aminopyridine³⁴. Subsequent bath application of NMDA produced an additional increase in ethidium fluorescence (Supplementary Fig. 3), suggesting that extrasynaptic NMDAR activation can also contribute to NADPH oxidase activation.

NMDAR activation of NOX involves PKC signaling

Protein kinase C (PKC) in neurons is activated by NMDAR activation^{35,36} and studies in other cell types have identified a role for PKC in the activation and membrane translocation of NADPH oxidase¹⁷. We examined the role of PKC in NMDA-induced NADPH oxidase activation using PKC isoform-specific peptide inhibitors. NMDA-induced superoxide formation was blocked by pre-treatment with a TAT-conjugated PKC ζ peptide inhibitor (1 μ M), but not by a TAT-conjugated PKC δ inhibitor or by the TAT carrier peptide alone (Fig. 4a,b). We used Fura-2 imaging to assess the possibility that the PKC ζ might directly or indirectly suppress NMDAR activity. Neurons treated with NMDA in the presence of the PKC peptide inhibitors showed no appreciable differences in their responses to Fura-2 (Supplementary Fig. 4 online), as previously reported³⁶.

We examined membrane translocation of p47^{phox}, a requisite step in NADPH oxidase activation, by immunostaining^{21,22}. p47^{phox} was distributed throughout the neuronal cytoplasm under basal conditions and was redistributed to the neuronal cell membrane on NMDAR activation (Fig. 4c,d). This redistribution was consistently blocked in cultures treated with the PKC ζ inhibitor, but not by the PKC δ inhibitor or TAT carrier peptide alone (Fig. 4c,d). p47^{phox} immunoreactivity was absent in p47^{phox}^{-/-} neurons and in cultures that were not incubated with antibody to p47^{phox} (data not shown).

Cultures exposed to NMDA for 30 min showed substantial neuronal death 24 h later, as evidenced by cytoplasmic membrane permeability to trypan blue (Fig. 5a,b). Neuronal death was reduced to control (wash only) values in cultures co-treated with the antioxidant Trolox, consistent with prior reports that identified superoxide as an important intermediate in NMDA excitotoxicity^{1,7}. Cell death was similarly reduced by drugs or conditions that blocked NADPH oxidase activity (apocynin, 6AN, PKC ζ inhibition and glucose-free medium) and in cultures prepared from p47^{phox}^{-/-} mice (Fig. 5). The p47^{phox}^{-/-} neurons did, however, retain their sensitivity to H₂O₂, thus excluding a nonspecific resistance to cell death. NMDA neurotoxicity was not reduced by the xanthine oxidase inhibitors allopurinol or gallic acid (Supplementary Fig. 2), which is consistent with the lack of effect of these compounds on NMDA-induced superoxide production. In contrast, L-NAME reduced neuronal cell death (Supplementary Fig. 2), consistent with prior studies linking nitric oxide production to NMDA excitotoxicity².

NOX inhibition blocks superoxide production *in vivo*

C57/Bl6 mice that were preloaded with dHEth and given NMDA injections into the hippocampus showed a robust increase in ethidium fluorescence in hippocampal neurons (Fig. 6). Mice that were injected with NMDA were also pre-treated with CNQX to block responses

that could occur as a result of NMDA-induced glutamate release on AMPA/kainate receptors; however, we obtained identical results from mice that were not injected with CNQX (data not shown). The NMDA-induced ethidium signal was markedly reduced in wild-type mice that were pretreated with apocynin and was almost eliminated in $p47^{phox-/-}$ mice (Fig. 6a,b). The ethidium signal was also reduced in mice treated with the peptide inhibitors for either PKC δ or PKC ζ , but not in those treated with the TAT carrier peptide (Fig. 6c,d).

Ethidium binds to nuclear DNA and thus does not provide the spatial localization of superoxide production. To better delineate the sites of superoxide production, we immunostained mouse hippocampal sections for 4HNE following stereotactic NMDA injections. 4HNE was formed in both the cell bodies and proximal dendrites of the wild-type hippocampal pyramidal neurons, with little 4HNE formation occurring in $p47^{phox-/-}$ mice (Fig. 7).

In a separate set of experiments, we maintained mice for 3 d following NMDA injections to examine the effects of NADPH oxidase inhibition on NMDA neurotoxicity in brain. Fluoro-Jade B staining revealed extensive neuronal degeneration in hippocampi injected with NMDA (Fig. 6e,f). Consistent with our ethidium fluorescence results, the NMDA-induced neurodegeneration was markedly reduced in wild-type mice treated with apocynin and in $p47^{phox-/-}$ mice.

DISCUSSION

These results provide four lines of evidence supporting NADPH oxidase as the primary source of NMDA-induced superoxide production in neurons. First, inhibition of NADPH oxidase with apocynin blocked the oxidation of dHEth, the formation of 4HNE and the neuronal death that otherwise resulted from NMDAR activation. Second, $p47^{phox-/-}$ neurons, which do not form a functional NOX2 NADPH oxidase complex, also showed a near-complete absence of these responses to NMDA. Third, glucose is specifically required to fuel NADPH regeneration through the hexose monophosphate shunt, and when we blocked flux through this pathway with either glucose-free medium or 6AN, we found reduced dHEth oxidation, 4HNE formation and neuronal death. Fourth, neurons treated with a peptide inhibitor of PKC ζ , which is involved in $p47^{phox}$ phosphorylation and NADPH oxidase activation³⁷, showed reduced membrane translocation of $p47^{phox}$, reduced superoxide formation and reduced cell death after NMDA exposures. We corroborated these cell culture results with experiments using NMDA injections into mouse hippocampus *in situ*; NMDA injections induced neuronal superoxide production and subsequent neuronal death and these were prevented by apocynin, $p47^{phox}$ gene deficiency and PKC ζ inhibition.

Our cell culture results indicate that superoxide is generated by neurons after NMDAR activation and our *in vivo* studies found that the ethidium signal was localized to the CA1 neuronal pyramidal layer after hippocampal injection of NMDA. We cannot formally exclude the possibility that other cell types such as microglia may contribute to the superoxide that we detected in the neurons *in vivo*, but non-neuronal cell types are distributed diffusely throughout the hippocampus and would therefore be unlikely to contribute to the ethidium signal, which was confined to the CA1 pyramidal layer. In addition, non-neuronal cells have little or no NMDAR activity, and brain harvest at 30 min after NMDA injections precludes the possibility of an astrocyte or microglial inflammatory response to neuronal cell death.

Prior studies have suggested that mitochondria are a primary source of NMDA-induced superoxide production on the basis of mitochondrial localization of oxidant-sensitive fluorescent indicators and a reduction in this mitochondrial signal with mitochondrial inhibitors^{10,11,15,38}. However, the localization of oxidized dyes to the mitochondria does not itself establish that mitochondria are the source of oxidant production, as demonstrated by

oxidation of mitoSOX in neuronal mitochondria by xanthine/xanthine oxidase added to the culture medium³⁹. A reduced fluorescent signal in response to mitochondrial inhibitors is therefore insufficient to establish mitochondria as the oxidant source, as these inhibitors also cause mitochondrial and plasma membrane depolarization, with the resultant dye efflux¹⁶. We used an alternative approach to identify mitochondrial superoxide production, which was based on the ability of non-glucose substrates such as pyruvate to support mitochondrial respiration. In our experiments, the lack of an NMDA-induced ethidium signal in cultures supplied with pyruvate in place of glucose provided independent evidence that mitochondria are not the primary source of NMDA induced superoxide production. In addition, neurons prepared from *Sod2*⁺ mice showed no reduction in the NMDA-induced ethidium signal, despite the fact that these neurons have a twofold increase in mitochondrial superoxide dismutase expression²⁹ and have an increased capacity to scavenge superoxide production induced by the mitochondrial complex III inhibitor antimycin.

Evidence for cross-talk between mitochondria and NADPH oxidase has been reported in non-neuronal cell types⁴⁰. The possibility that a small superoxide signal originating in the mitochondria could trigger a larger superoxide production by NADPH oxidase could reconcile our results with those of prior studies that have suggested a major role for mitochondria in NMDA-induced neuronal superoxide production. However, the undiminished superoxide signal observed in both *Sod2*⁺ neurons (Fig. 3h) and wild-type neurons treated with inhibitors of substrate flux to the mitochondria (Supplementary Fig. 1) argues against this scenario. Alternatively, an initial superoxide signal produced by NADPH oxidase could induce an additional, secondary superoxide production from mitochondria. Mitochondria normally act as sinks for extra-mitochondrial sources of reactive oxygen species¹², but can become net generators of reactive oxygen species if their antioxidant mechanisms are impaired or overwhelmed. The undiminished superoxide production observed in *Sod2*⁺ neurons also weighs against mitochondria being a substantial secondary source of superoxide, but does not entirely exclude this possibility.

Superoxide that is produced by NADPH oxidase and other sources can be detected with dHEth^{10,19–22,41}. The oxidation of dHEth to 2-hydroxyethidium is highly specific for superoxide under cell-free conditions, but peroxidases that are present in living tissues can enable other oxidants, such as H₂O₂, to react with dHEth, either alone or in sequence with superoxide, to generate multiple fluorescent products with overlapping spectra^{19,20}. These other oxidants are derived from superoxide⁴², however, and our finding that the NMDA-induced ethidium signal was blocked by both Trolox and by pharmacologic or genetic ablation of NADPH oxidase activity provides confirming evidence that the ethidium signal that we detected is primarily attributable to superoxide or superoxide metabolites.

NMDAR activation gates a large calcium influx, and this calcium influx has been definitively linked to both superoxide production^{10,38} and NMDA neurotoxicity⁴³. Calcium influx is also a strong stimulus for NADPH oxidase activation. Intracellular Ca²⁺ elevations activate PKC, which in turn phosphorylates p47^{phox}, the organizer subunit of NOX2 (ref. 17). The phosphorylation of p47^{phox} triggers its assembly with the other NOX2 subunits and translocation to the membrane as an activated enzyme complex^{17,44}. Several PKC isoforms, including PKC ζ and PKC δ , have been found to participate in p47^{phox} phosphorylation and NOX2 activation in different cell types^{37,45}. Our findings indicate that PKC ζ is the primary isoform that is responsible for p47^{phox} translocation and NOX activation in cortical neurons cultures, but also suggest that PKC δ may contribute to this process in both neuron cultures and hippocampal pyramidal neurons *in situ*. Both PKC ζ and PKC δ have been shown to mediate neuronal death induced by NMDAR activation and ischemia^{36,46,47}, and our results thus provide a potential mechanism for these effects. These results also suggest a mechanism by

which PKC ζ can facilitate long-term potentiation⁴⁸, in which glutamate-induced superoxide formation is a contributing factor^{4,5}.

Our results identify a dominant role for NADPH oxidase in NMDAR-mediated superoxide formation, but these results do not negate the potential for mitochondrial superoxide production in other settings. Conversely, NADPH oxidase in neurons and other cell types may also be activated by mechanisms independent of NMDAR activation. Our finding that NMDAR stimulation triggers NADPH oxidase activation provides a mechanistic link between excitotoxicity and oxidative stress and suggests that targeting neuronal NADPH oxidase may be an effective way to influence these NMDAR-mediated processes.

Supplementary Material

Refer to Web version on PubMed Central for supplementary material.

ACKNOWLEDGMENTS

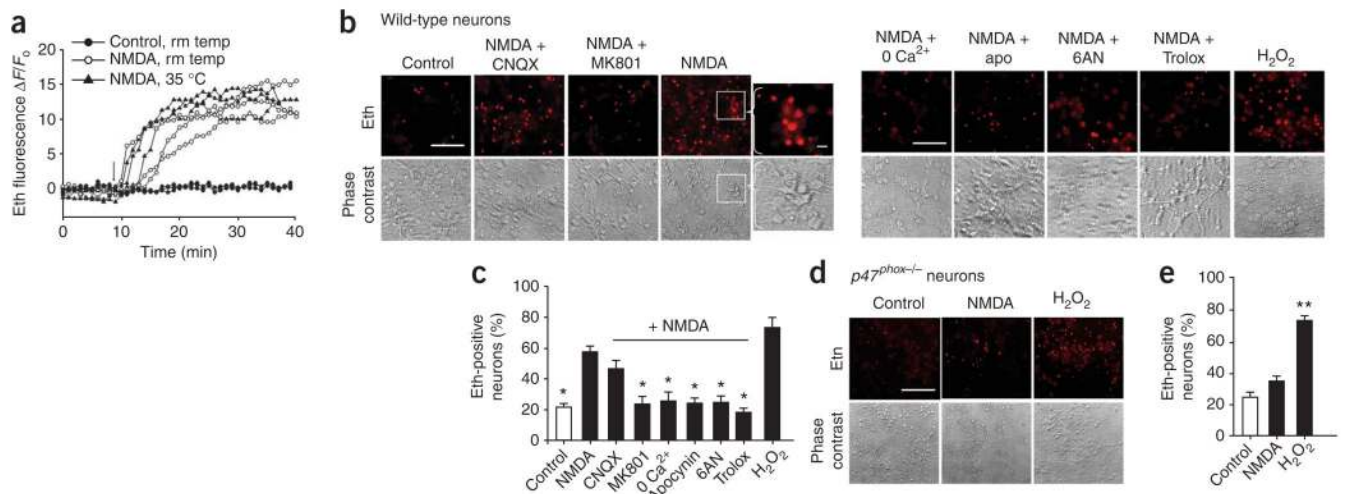
We thank D. Mochly-Rosen for advice with the TAT-conjugated peptides, C. Alano and C. Escartin for their careful reviews of the manuscript, and C. Hefner for technical assistance. This work was supported by the Department of Veterans Affairs Merit Review program (R.A.S.) and by the US National Institutes of Health (grants NS14543 to P.H.C. and NS051855 and NS051855 to R.A.S.).

References

1. Lafon-Cazal M, Pietri S, Culcasi M, Bockaert J. NMDA-dependent superoxide production and neurotoxicity. *Nature* 1993;364:535–537. [PubMed: 7687749]
2. Mandir AS, et al. NMDA, but not non-NMDA, excitotoxicity is mediated by poly(ADP-ribose) polymerase. *J. Neurosci* 2000;20:8005–8011. [PubMed: 11050121]
3. MacDermott AB, Mayer ML, Westbrook GL, Smith SJ, Barker JL. NMDA receptor activation increases cytoplasmic calcium concentration in cultured spinal cord neurones. *Nature* 1986;321:519–522. [PubMed: 3012362]
4. Klann E. Cell-permeable scavengers of superoxide prevent long-term potentiation in hippocampal area CA1. *J. Neurophysiol* 1998;80:452–457. [PubMed: 9658063]
5. MacDonald JF, Jackson MF, Beazely MA. Hippocampal long-term synaptic plasticity and signal amplification of NMDA receptors. *Crit. Rev. Neurobiol* 2006;18:71–84. [PubMed: 17725510]
6. Aizenman E, Hartnett KA, Reynolds IJ. Oxygen free radicals regulate NMDA receptor function via a redox modulatory site. *Neuron* 1990;5:841–846. [PubMed: 2148489]
7. Patel M, Day BJ, Crapo JD, Fridovich I, McNamara JO. Requirement for superoxide in excitotoxic cell death. *Neuron* 1996;16:345–355. [PubMed: 8789949]
8. White RJ, Reynolds IJ. Mitochondrial depolarization in glutamate-stimulated neurons: an early signal specific to excitotoxin exposure. *J. Neurosci* 1996;16:5688–5697. [PubMed: 8795624]
9. Budd SL, Nicholls DG. Mitochondria, calcium regulation and acute glutamate excitotoxicity in cultured cerebellar granule cells. *J. Neurochem* 1996;67:2282–2291. [PubMed: 8931459]
10. Bindokas VP, Jordan J, Lee CC, Miller RJ. Superoxide production in rat hippocampal neurons: selective imaging with hydroethidine. *J. Neurosci* 1996;16:1324–1336. [PubMed: 8778284]
11. Dugan LL, et al. Mitochondrial production of reactive oxygen species in cortical neurons following exposure to *N*-methyl-D-aspartate. *J. Neurosci* 1995;15:6377–6388. [PubMed: 7472402]
12. Andreyev AY, Kushnareva YE, Starkov AA. Mitochondrial metabolism of reactive oxygen species. *Biochemistry (Mosc.)* 2005;70:200–214. [PubMed: 15807660]
13. Adam-Vizi V, Chinopoulos C. Bioenergetics and the formation of mitochondrial reactive oxygen species. *Trends Pharmacol. Sci* 2006;27:639–645. [PubMed: 17056127]
14. Dykens JA. Isolated cerebral and cerebellar mitochondria produce free radicals when exposed to elevated Ca²⁺ and Na⁺: implications for neurodegeneration. *J. Neurochem* 1994;63:584–591. [PubMed: 8035183]

15. Duan Y, Gross RA, Sheu SS. Ca^{2+} -dependent generation of mitochondrial reactive oxygen species serves as a signal for poly(ADP-ribose) polymerase-1 activation during glutamate excitotoxicity. *J. Physiol. (Lond.)* 2007;585:741–758. [PubMed: 17947304]
16. Nicholls DG. Simultaneous monitoring of ionophore- and inhibitor-mediated plasma and mitochondrial membrane potential changes in cultured neurons. *J. Biol. Chem* 2006;281:14864–14874. [PubMed: 16551630]
17. Bedard K, Krause KH. The NOX family of ROS-generating NADPH oxidases: physiology and pathophysiology. *Physiol. Rev* 2007;87:245–313. [PubMed: 17237347]
18. Tejada-Simon MV, et al. Synaptic localization of a functional NADPH oxidase in the mouse hippocampus. *Mol. Cell. Neurosci* 2005;29:97–106. [PubMed: 15866050]
19. Robinson KM, et al. Selective fluorescent imaging of superoxide *in vivo* using ethidium-based probes. *Proc. Natl. Acad. Sci. USA* 2006;103:15038–15043. [PubMed: 17015830]
20. Zhao H, et al. Superoxide reacts with hydroethidine, but forms a fluorescent product that is distinctly different from ethidium: potential implications in intracellular fluorescence detection of superoxide. *Free Radic. Biol. Med* 34;2003:1359–1368.
21. Suh SW, Gum ET, Hamby AM, Chan PH, Swanson RA. Hypoglycemic neuronal death is triggered by glucose reperfusion and activation of neuronal NADPH oxidase. *J. Clin. Invest* 2007;117:910–918. [PubMed: 17404617]
22. Suh SW, et al. Glucose and NADPH oxidase drive neuronal superoxide formation in stroke. *Ann. Neurol* 2008;64:654–663. [PubMed: 19107988]
23. Stolk J, Hiltermann TJ, Dijkman JH, Verhoeven AJ. Characteristics of the inhibition of NADPH oxidase activation in neutrophils by apocynin, a methoxy-substituted catechol. *Am. J. Respir. Cell Mol. Biol* 1994;11:95–102. [PubMed: 8018341]
24. Bender JG, Van Epps DE. Inhibition of human neutrophil function by 6-aminonicotinamide: the role of the hexose monophosphate shunt in cell activation. *Immunopharmacology* 1985;10:191–199. [PubMed: 3009354]
25. Gupte SA, et al. Glucose-6-phosphate dehydrogenase-derived NADPH fuels superoxide production in the failing heart. *J. Mol. Cell. Cardiol* 2006;41:340–349. [PubMed: 16828794]
26. Inanami O, et al. Activation of the leukocyte NADPH oxidase by phorbol ester requires the phosphorylation of p47PHOX on serine 303 or 304. *J. Biol. Chem* 1998;273:9539–9543. [PubMed: 9545283]
27. Uchida K. 4-Hydroxy-2-nonenal: a product and mediator of oxidative stress. *Prog. Lipid Res* 2003;42:318–343. [PubMed: 12689622]
28. Lai B, et al. Inhibition of Qi site of mitochondrial complex III with antimycin A decreases persistent and transient sodium currents via reactive oxygen species and protein kinase C in rat hippocampal CA1 cells. *Exp. Neurol* 2005;194:484–494. [PubMed: 16022873]
29. Raineri I, et al. Strain-dependent high-level expression of a transgene for manganese superoxide dismutase is associated with growth retardation and decreased fertility. *Free Radic. Biol. Med* 2001;31:1018–1030. [PubMed: 11595386]
30. Abramov AY, Scorziello A, Duchon MR. Three distinct mechanisms generate oxygen free radicals in neurons and contribute to cell death during anoxia and reoxygenation. *J. Neurosci* 2007;27:1129–1138. [PubMed: 17267568]
31. Porasuphatana S, Tsai P, Rosen GM. The generation of free radicals by nitric oxide synthase. *Comp. Biochem. Physiol. C Toxicol. Pharmacol* 2003;134:281–289. [PubMed: 12643975]
32. Cheng Y, Sun AY. Oxidative mechanisms involved in kainate-induced cytotoxicity in cortical neurons. *Neurochem. Res* 1994;19:1557–1564. [PubMed: 7877729]
33. Atlante A, et al. Glutamate neurotoxicity in rat cerebellar granule cells: a major role for xanthine oxidase in oxygen radical formation. *J. Neurochem* 1997;68:2038–2045. [PubMed: 9109530]
34. Hardingham GE, Fukunaga Y, Bading H. Extrasynaptic NMDARs oppose synaptic NMDARs by triggering CREB shut-off and cell death pathways. *Nat. Neurosci* 2002;5:405–414. [PubMed: 11953750]
35. Favaron M, et al. Down-regulation of protein kinase C protects cerebellar granule neurons in primary culture from glutamate-induced neuronal death. *Proc. Natl. Acad. Sci. USA* 1990;87:1983–1987. [PubMed: 1689850]

36. Koponen S, et al. Prevention of NMDA-induced death of cortical neurons by inhibition of protein kinase C zeta. *J. Neurochem* 2003;86:442–450. [PubMed: 12871585]
37. Dang PM, Fontayne A, Hakim J, El Benna J, Perianin A. Protein kinase C zeta phosphorylates a subset of selective sites of the NADPH oxidase component p47phox and participates in formyl peptide-mediated neutrophil respiratory burst. *J. Immunol* 2001;166:1206–1213. [PubMed: 11145703]
38. Reynolds IJ, Hastings TG. Glutamate induces the production of reactive oxygen species in cultured forebrain neurons following NMDA receptor activation. *J. Neurosci* 1995;15:3318–3327. [PubMed: 7751912]
39. Johnson-Cadwell LI, Jekabsons MB, Wang A, Polster BM, Nicholls DG. ‘Mild Uncoupling’ does not decrease mitochondrial superoxide levels in cultured cerebellar granule neurons, but decreases spare respiratory capacity and increases toxicity to glutamate and oxidative stress. *J. Neurochem* 2007;101:1619–1631. [PubMed: 17437552]
40. Brandes RP. Triggering mitochondrial radical release: a new function for NADPH oxidases. *Hypertension* 2005;45:847–848. [PubMed: 15837827]
41. Chan PH, et al. Overexpression of SOD1 in transgenic rats protects vulnerable neurons against ischemic damage after global cerebral ischemia and reperfusion. *J. Neurosci* 1998;18:8292–8299. [PubMed: 9763473]
42. Fernandes DC, et al. Analysis of DHE-derived oxidation products by HPLC in the assessment of superoxide production and NADPH oxidase activity in vascular systems. *Am. J. Physiol. Cell Physiol* 2007;292:C413–C422. [PubMed: 16971501]
43. Hyrc K, Handran SD, Rothman SM, Goldberg MP. Ionized intracellular calcium concentration predicts excitotoxic neuronal death: observations with low-affinity fluorescent calcium indicators. *J. Neurosci* 1997;17:6669–6677. [PubMed: 9254679]
44. Clark RA, Volpp BD, Leidal KG, Nauseef WM. Two cytosolic components of the human neutrophil respiratory burst oxidase translocate to the plasma membrane during cell activation. *J. Clin. Invest* 1990;85:714–721. [PubMed: 2155923]
45. Bey EA, et al. Protein kinase C delta is required for p47phox phosphorylation and translocation in activated human monocytes. *J. Immunol* 2004;173:5730–5738. [PubMed: 15494525]
46. Bright R, et al. Protein kinase C delta mediates cerebral reperfusion injury *in vivo*. *J. Neurosci* 2004;24:6880–6888. [PubMed: 15295022]
47. Crisanti P, Leon A, Lim DM, Omri B. Aspirin prevention of NMDA-induced neuronal death by direct protein kinase Czeta inhibition. *J. Neurochem* 2005;93:1587–1593. [PubMed: 15935075]
48. Sacktor TC. PKMzeta, LTP maintenance and the dynamic molecular biology of memory storage. *Prog. Brain Res* 2008;169:27–40. [PubMed: 18394466]
49. Ying W, et al. Differing effects of copper, zinc superoxide dismutase overexpression on neurotoxicity elicited by nitric oxide, reactive oxygen species and excitotoxins. *J. Cereb. Blood Flow Metab* 2000;20:359–368. [PubMed: 10698074]

**Figure 1.**

NADPH oxidase is the major source of NMDA-induced superoxide formation in neurons.

(a) Traces show ethidium (eth) fluorescence over time, as measured in individual neurons preloaded with dHEth. Following baseline fluorescence recording, neurons were treated with 100 μ M NMDA (arrow) at either 21–25 °C or 35 °C. Traces are representative of >40 neurons under each condition from four independent studies. (b) Ethidium fluorescence and corresponding phase contrast images of cortical neuron cultures photographed 30 min after incubation with NMDA (100 μ M) alone or with MK801 (10 μ M), CNQX (10 μ M), apocynin (apo, 500 μ M), 6AN (500 μ M) or Trolox (100 μ M). For calcium-free experiments, neurons were incubated with a zero-calcium buffer and 1 mM EGTA. Control wells received medium exchanges only. H₂O₂ (100 μ M) served as a positive control. Inset, higher magnification of ethidium-positive neurons from the region indicated by the white box. Scale bar represents 10 μ m. (c) Quantification of ethidium-positive neurons under the conditions shown in b. (d) Ethidium fluorescence and corresponding phase-contrast images of *p47^{phox-/-}* neurons incubated with NMDA (100 μ M) or H₂O₂ (100 μ M). Scale bar represents 10 μ m. (e) Quantification of ethidium-positive neurons under the conditions shown in d. * $P < 0.05$ and ** $P < 0.01$ versus NMDA alone ($n \geq 3$). Error bars indicate s.e.m.

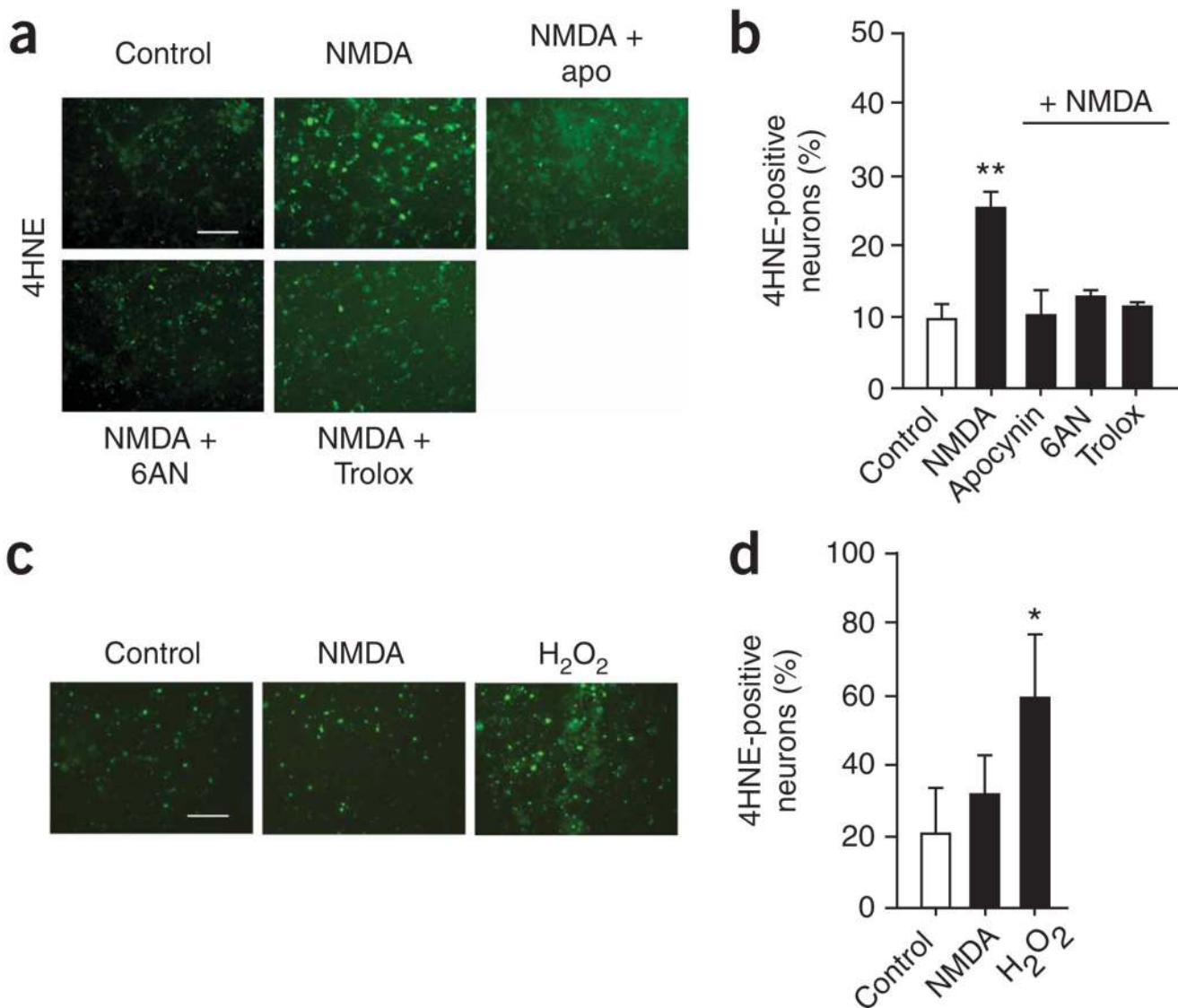


Figure 2. NMDA-induced oxidative damage was prevented by NADPH oxidase inhibition. (**a-d**) Immunostaining for 4HNE in wild-type (**a**) and *p47^{phox}-/-* (**c**) neuron cultures (conditions as described in Fig. 1). 4HNE immunostaining is quantified in **b** and **d** for **a** and **c**, respectively. * $P < 0.05$ and ** $P < 0.01$ versus control ($n = 3$). Scale bars represent 10 μm . Error bars indicate s.e.m.

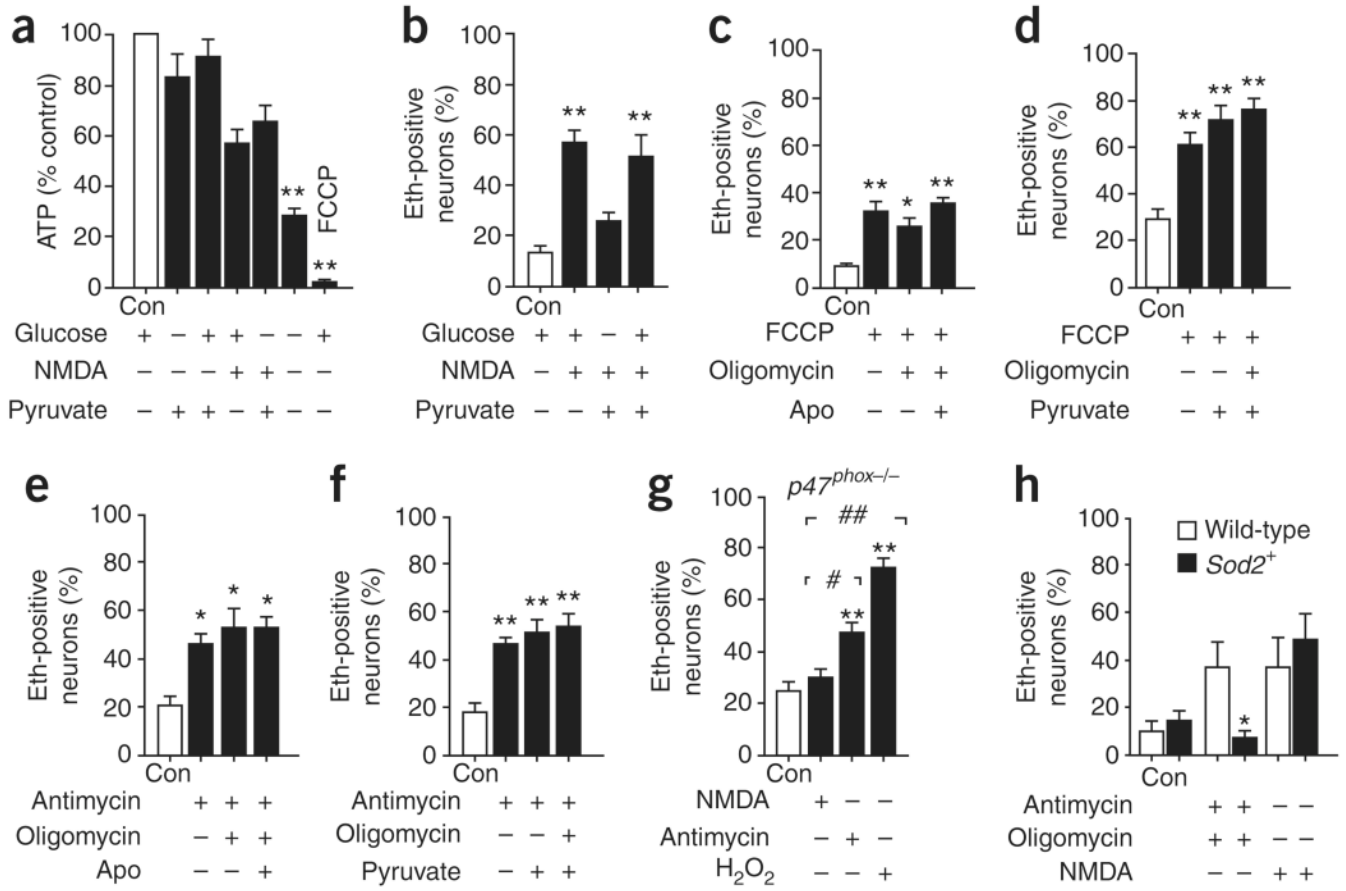


Figure 3. Mitochondria do not substantially contribute to NMDA-induced superoxide production. **(a)** We found comparable ATP levels in neurons incubated with 5 mM glucose or 1 mM pyruvate, confirming that mitochondrial respiration is supported by pyruvate. ATP levels were reduced by the absence of both substrates or by the presence of FCCP (3 μ M). **(b)** Glucose was required for NMDA-induced superoxide production and this was not suppressed by pyruvate (500 μ M). **(c-g)** The ethidium fluorescence method detected mitochondrial superoxide produced by neurons incubated with FCCP (3 μ M, **c,d**) or with the complex III inhibitor antimycin (3 μ M, **e,f**), with or without 3 μ M oligomycin. This mitochondrial ethidium signal was not attenuated by 500 μ M apocynin or pyruvate (**c-f**) or in *p47^{phox}-/-* neurons (**g**). **(h)** Neurons prepared from *Sod2⁺* mice had an attenuated ethidium response to antimycin and oligomycin relative to wild-type littermates, but had no reduction in ethidium increase following NMDA application. * $P < 0.05$ and ** $P < 0.01$ versus control, # $P < 0.05$ and ### $P < 0.01$ versus NMDA ($n \geq 3$). Error bars indicate s.e.m.

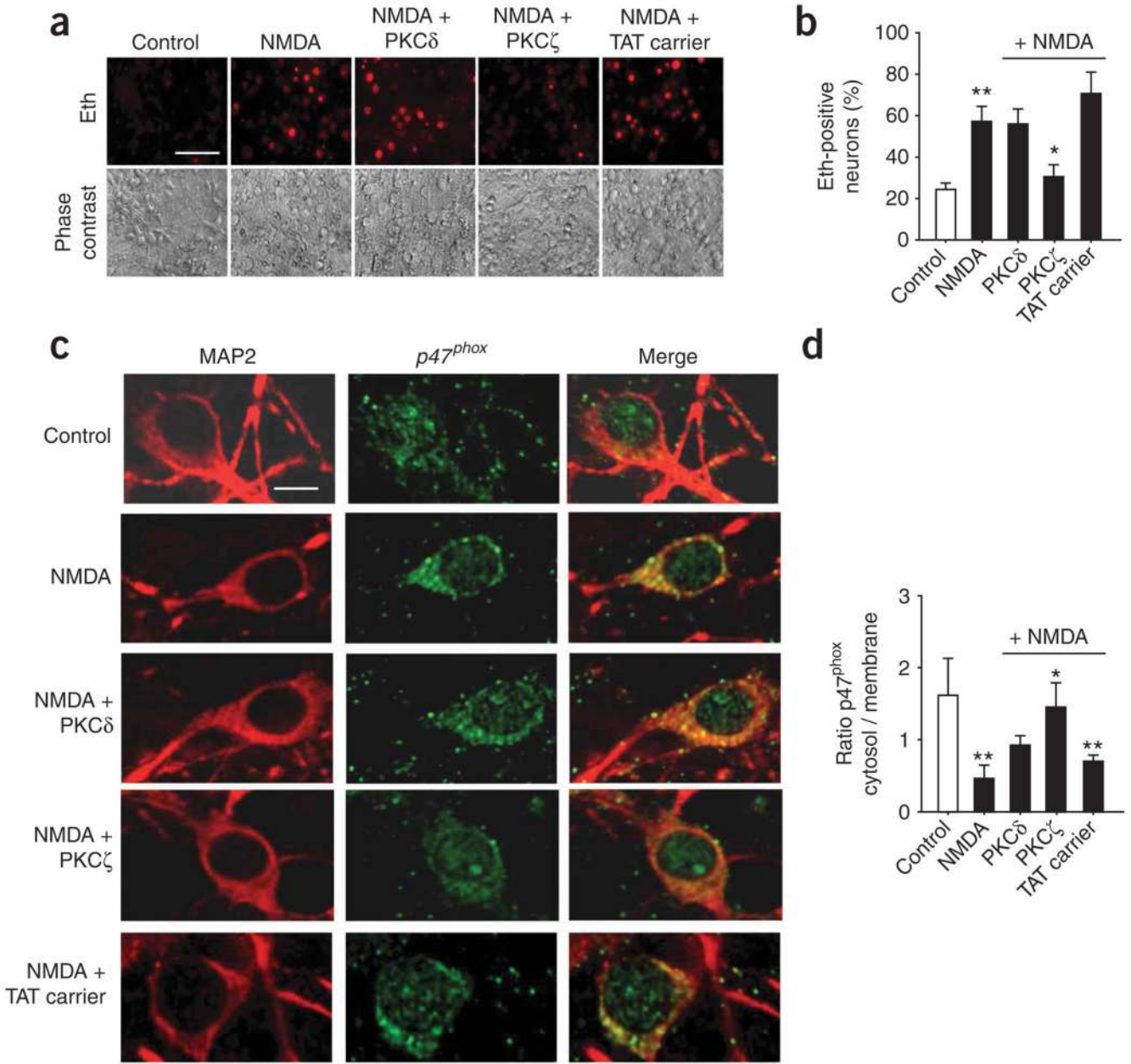


Figure 4. NMDA activation of NADPH oxidase is mediated by PKC. **(a)** Ethidium fluorescence and corresponding phase-contrast images of cortical neuron cultures photographed 30 min after incubation with NMDA (100 μ M) alone or with the peptide inhibitors PKC δ , PKC ζ , or TAT carrier peptide (all 1 μ M). Scale bar represents 10 μ m. **(b)** Quantification of Eth fluorescence. **(c)** Immunostaining for p47^{phox} and MAP2 in neurons indicated that NMDA-induced translocation of the p47^{phox} subunit to the cell membrane was attenuated by the PKC ζ peptide inhibitor. Scale bar represents 2 μ m. **(d)** Quantification of p47^{phox} membrane translocation. * $P < 0.05$ versus NMDA and ** $P < 0.05$ versus control ($n \geq 4$). Error bars indicate s.e.m.

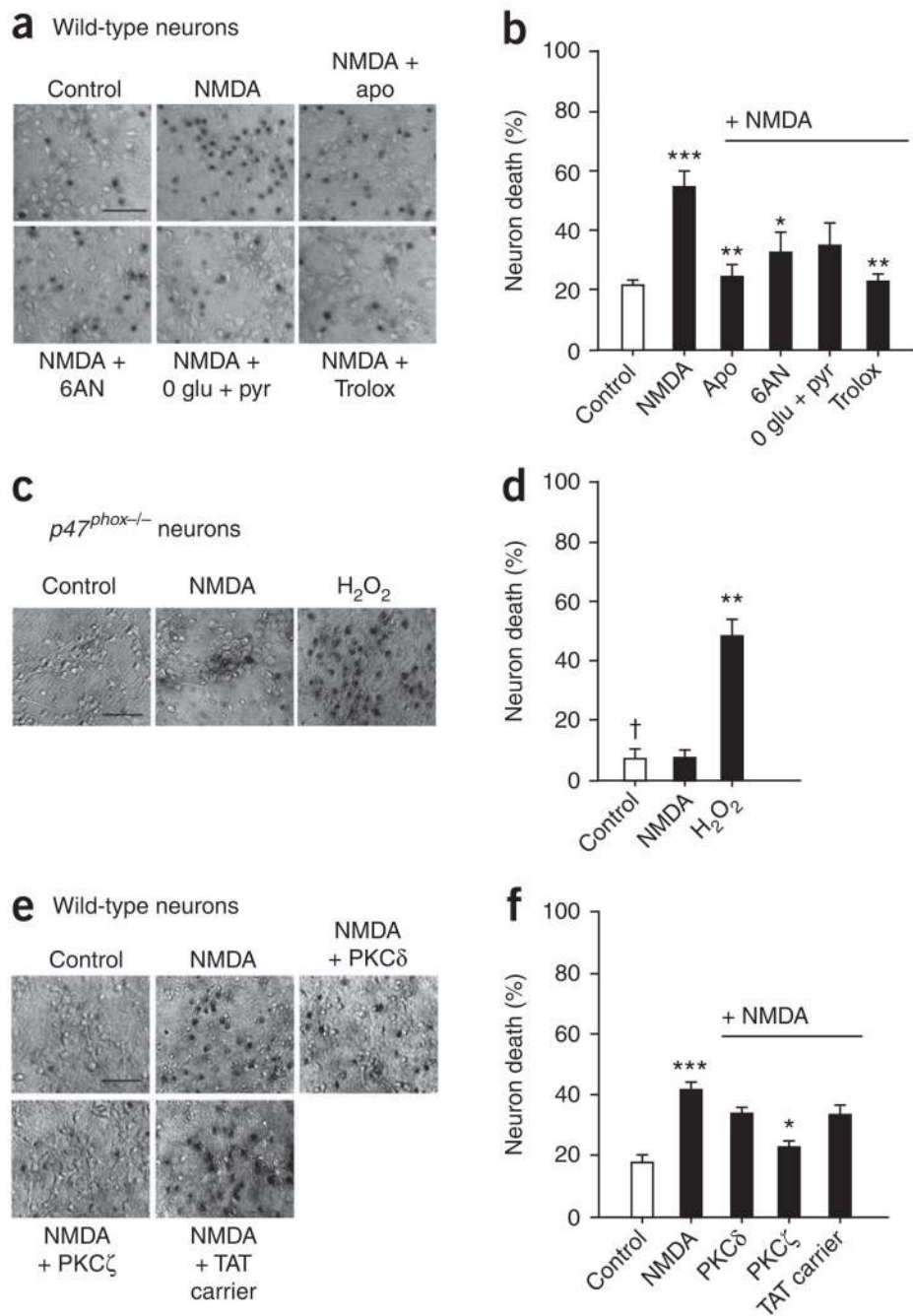


Figure 5. Inhibition of NADPH oxidase prevents NMDA-induced cell death. (**a–f**) Dead neurons were identified with trypan blue staining 24 h after NMDA incubations. 0 glu + pyr indicates glucose-free medium with 1 mM pyruvate. All other conditions are as described in Figure 1 and Figure 3. Neuronal death is quantified in **b**, **d** and **f** for **a**, **c** and **e**, respectively. Scale bar = 40 μ m. * $P < 0.05$ and ** $P < 0.01$ versus NMDA, *** $P < 0.05$ versus control, and † $P < 0.05$ versus wild-type NMDA ($n = 4$). Error bars indicate s.e.m.

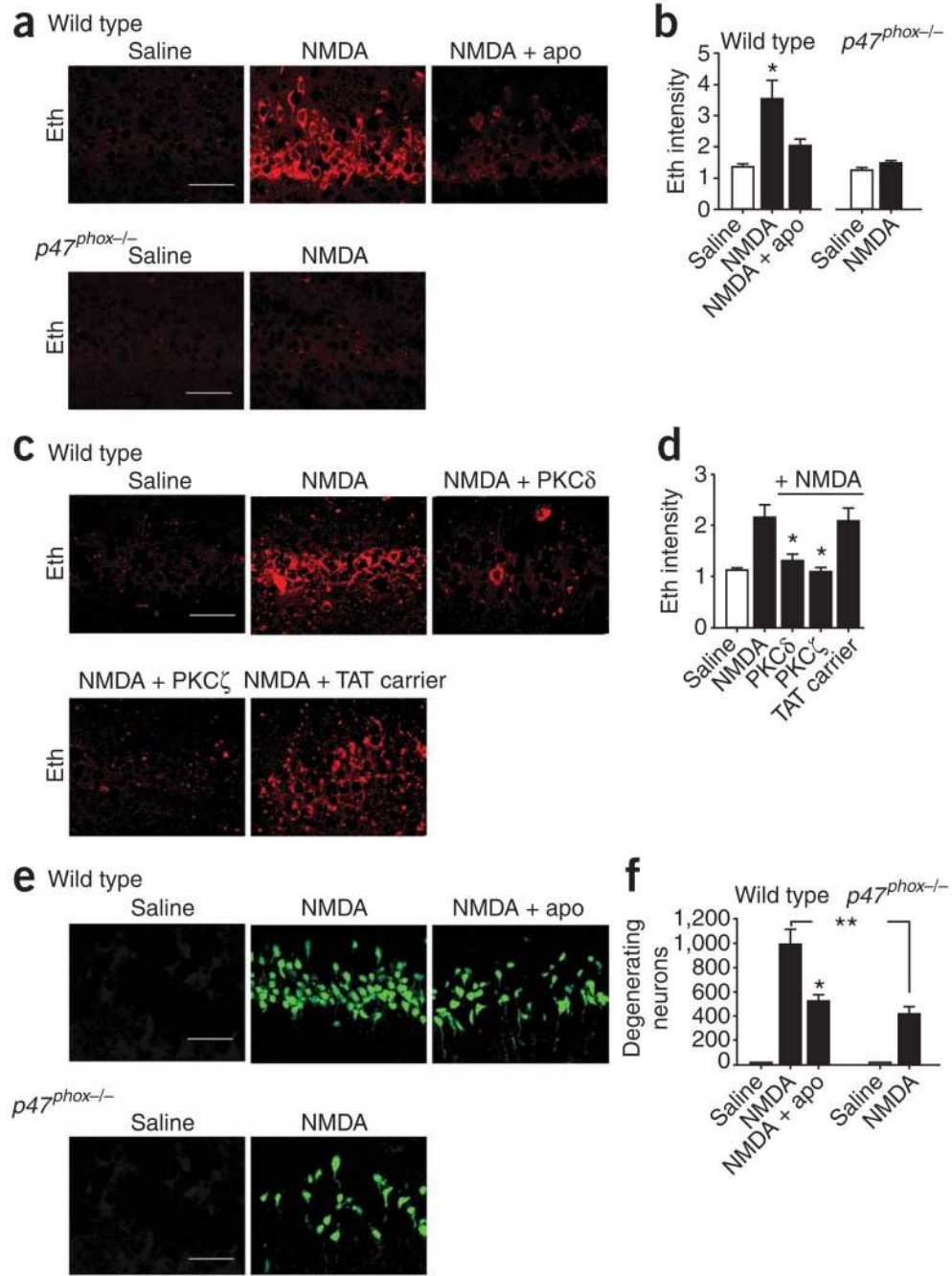


Figure 6. NMDA induced superoxide in mouse hippocampus. **(a)** Representative images of ethidium fluorescence in neurons from the CA1 hippocampus of wild-type or *p47^{phox}-/-* mice. Tissue was harvested 30 min after NMDA injections. **(b)** Comparison of ethidium intensity between groups. **(c)** Representative images of NMDA-induced ethidium fluorescence in neurons from the CA1 hippocampus of wild-type mice pre-treated with peptide inhibitors of PKC δ and PKC ζ or the TAT carrier peptide. **(d)** Quantification of ethidium intensity between groups. **(e)** Representative images of degenerating neurons, stained with Fluoro-Jade B in the CA1 hippocampus of wild-type or *p47^{phox}-/-* mice 3 d after NMDA injections. **(f)** Quantification

of Fluoro-Jade B–positive neurons. Scale bars represent 50 μm . * $P < 0.05$ ($n = 4$). Error bars indicate s.e.m.

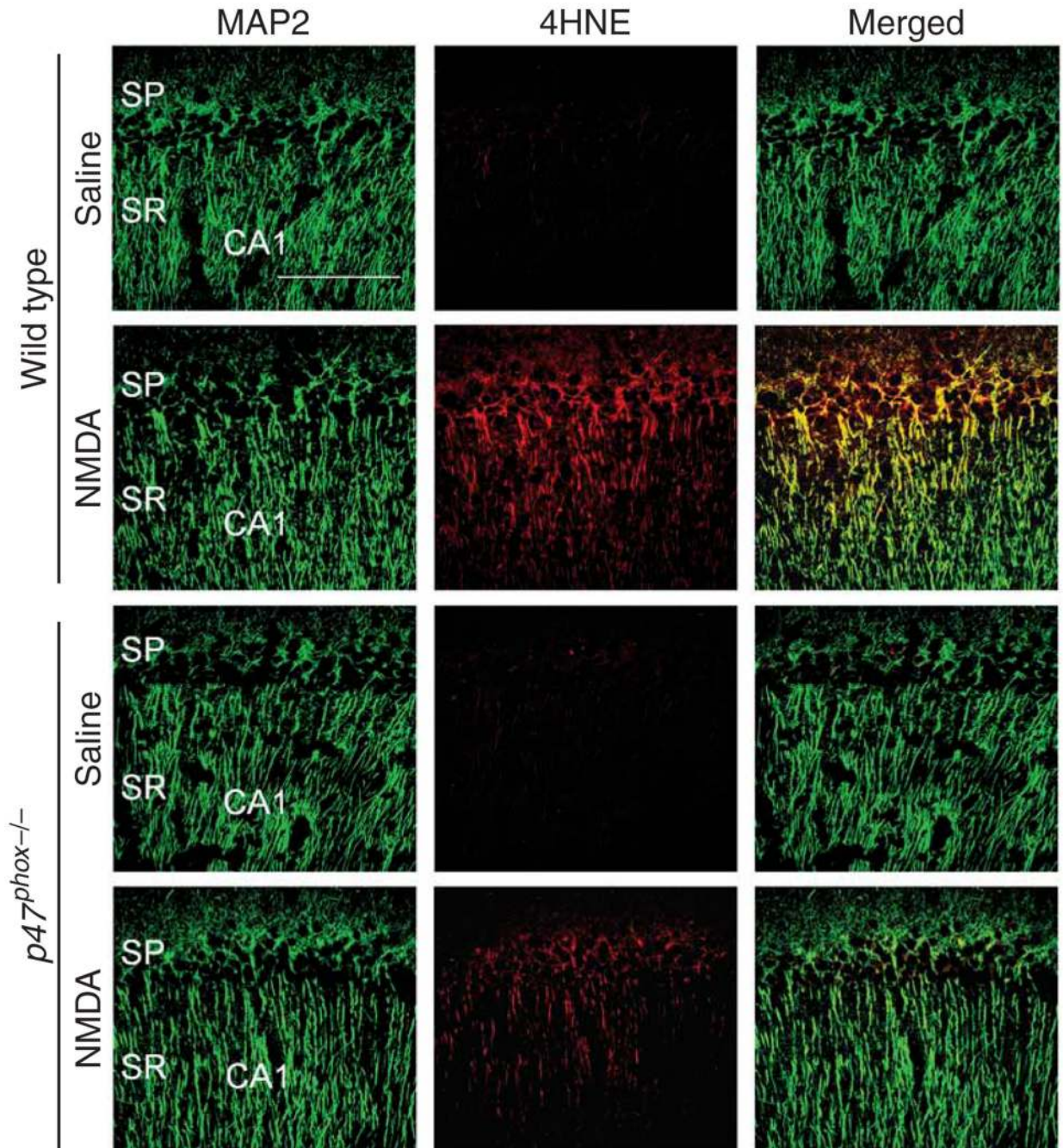


Figure 7.

NMDA-induced superoxide production in cell bodies and dendrites. Confocal images of mouse CA1 hippocampus after immunostaining for the neuronal marker MAP2 and the lipid oxidation product 4HNE. Brains were harvested 30 min after stereotactic injections with NMDA. 4HNE formation was evident in the neuronal cell bodies of the stratum pyramidale (SP) and in the dendrites extending from the stratum radiatum (SR). 4HNE formation was markedly reduced in $p47^{phox-/-}$ mice. Scale bar represents 40 μm . Images are representative of three mice from each group.